Geocarto International

ISSN: (Print) (Online) Journal homepage: https://www.tandfonline.com/loi/tgei20

Use of multi-source remotely sensed data in monitoring the spatial distribution of pools and pool dynamics along non-perennial rivers in semi-arid environments, South Africa

S. E. Maswanganye, T. Dube, N. Jovanovic & D. Mazvimavi

To cite this article: S. E. Maswanganye, T. Dube, N. Jovanovic & D. Mazvimavi (2022) Use of multi-source remotely sensed data in monitoring the spatial distribution of pools and pool dynamics along non-perennial rivers in semi-arid environments, South Africa, Geocarto International, 37:25, 10970-10989, DOI: 10.1080/10106049.2022.2043453

To link to this article: https://doi.org/10.1080/10106049.2022.2043453

GEOCARTO INTERNATIONAL
2022, VOL. 37, NO. 25, 10970–10989
https://doi.org/10.1080/10106049.2022.2043453

Taylor & Francis
Taylor & Francis Group

Use of multi-source remotely sensed data in monitoring the spatial distribution of pools and pool dynamics along non-perennial rivers in semi-arid environments, South Africa

S. E. Maswanganye, T. Dube, N. Jovanovic and D. Mazvimavi

Institute for Water Studies, University of the Western Cape, Bellville, South Africa

ABSTRACT

This study explored the use of multi-source remotely sensed data in monitoring the spatial distribution of pools and pool dynamics in two distinct semi-arid sites in South Africa. The factors that control the pool dynamics were also examined. Three water extraction indices were used, these included Normalised Difference Water Index (NDWI), Modified NDWI and Normalised Difference Vegetation Index. In addition, random forest classifier and Sentinel-1 SAR data were used in mapping pools and pools dynamics for both sites. Overall, the remotely-sensed methods detected and mapped pools with acceptable accuracy, except for small pools ($<400\,m^2$). The results suggest that flow occurrences and rainfall are key in controlling temporal changes in pools sizes, and there was no interaction between pools and groundwater. The study showed that remote sensing methods are essential for filling ground monitoring gaps in non-perennial rivers and determining hydrological processes and water availability from pools in semi-arid environments.

ARTICLE HISTORY
Received 20 October 2021
Accepted 12 February 2022

KEYWORDS
Dryland pools; ephemeral streams; pool dynamics; remote sensing; water resource management

1. Introduction

Non-perennial rivers (NPRs) are characterised by the lack of flows for varying periods during the year. Some of these rivers will also have permanent or temporary pools not connected by flows. These pools are one of the most distinguishing features of NPRs (Hughes 2005; Datry et al. 2017), they are found worldwide and are expected to increase as NPRs expand (Grenfell et al. 2021) due to climate change and increased socio-economic uses. Zacharias and Zamparas (2010) defined pools as shallow water bodies that vary in depth, shape, and size, and are usually flooded from time to time and last long enough to sustain/support life.

Pools along NPRs are important water sources as they often provide water for livestock and domestic purposes in rural areas (Zamxaka et al. 2004; Peden et al. 2012; Naidoo et al. 2020). In addition, these resources provide ecohydrological services and indirectly support the tourism sector and livelihoods. Besides, they also act as habitats, feeding and

CONTACT S. E. Maswanganye 3031049@myuwc.ac.za

spawning ground for various aquatics species (Makwinja et al. 2014). There is a significant species-volume relationship in pools as species richness increases with size (Bonada et al. 2020). Species richness also depends on the physical-chemical properties of the pools. Pools attenuate floods (Liu and Zhang 2017) as they store floodwater (Datry et al. 2017) and are regarded as important zones of groundwater and surface water interactions (discharge and recharge zones).

Despite being important, pools along the NPRs are perceived to be of low value compared to perennial rivers (Rodríguez-Lozano et al. 2020), as they are considered an unreliable source of water. However, of late, pools along NPRs have received attention because of their ecological significance (Sheldon et al. 2010; Marshall et al. 2016; Ilhéu et al. 2020), hence also referred to as refugia or refuge, indicating their ecological importance as a habitat during the dry phase (Davis et al. 2013). Studies on the ecology of pools have suggested that they should be incorporated in river and water management. For instance, Groves et al. (2012) state that protecting these pools should be included in climate change adaptation plans. Importance of these pools is also recognised in most environmental flow assessments of NPRs as minimum water discharge is often maintained to ensure the persistence of pools during the dry period (Theodoropoulos et al. 2019).

Although pools are being recognised for their ecological importance, there is still limited scientific research on pools' hydrological and geomorphological aspects (Bonada et al. 2020; Bourke et al. 2020; Shanafield et al. 2021) due to limited in-situ monitoring sites along NPRs. Hence, monitoring is an essential step in understanding and managing pools effectively. However, monitoring of these pools using in-situ methods can be challenging as they can be sparsely distributed along the river (Maswanganye et al. 2021). The ability of remote sensing to distinguish between water and bare surfaces provides unique opportunities to monitor these pools both individually and at catchment scale. Seaton et al. (2020) demonstrated the potential of using multispectral remote sensing data (Sentinel-2 and Landsat 8) in monitoring the pool surface areas along NPRs with once-off validation. However, the study indicated that the number of observations was limited due to cloud cover over the study sites. Synthetic Aperture Radar (SAR) data such as Sentinel-1 can be used to overcome issues of cloudiness.

However, monitoring of pools without understanding factors influencing their distribution and occurrences remains inadequate for the sustainable management of these systems. So far, few studies have assessed controlling factors of pool storage dynamics across varying landscapes. For instance, Hamilton et al. (2005) investigated the persistency of pools using stable isotopes and major ions. The results showed that evaporative losses explained the changes in the pool's sizes between the flows, and there was no evidence of groundwater inputs into the pools. Using radon, Lamontagne et al. (2021) found that most pools were perennial and groundwater-fed in South Austria. Bestland et al. (2017) also made a similar observation in South Austria, however they added that the interaction between pools and groundwater may be seasonal, not a continuous water supply from groundwater to pools.

This study aimed at determining the spatial and temporal distribution of pools in two contrasting non-perennial rivers located in semi-arid environments (Touws and Molototsi Rivers in South Africa). This was done through (i) detection of pools along reaches of non-perennial rivers, (ii) accuracy assessment of remotely-sensed pool's surface area, (iii) determination of changes in pool sizes and factors that control these changes.

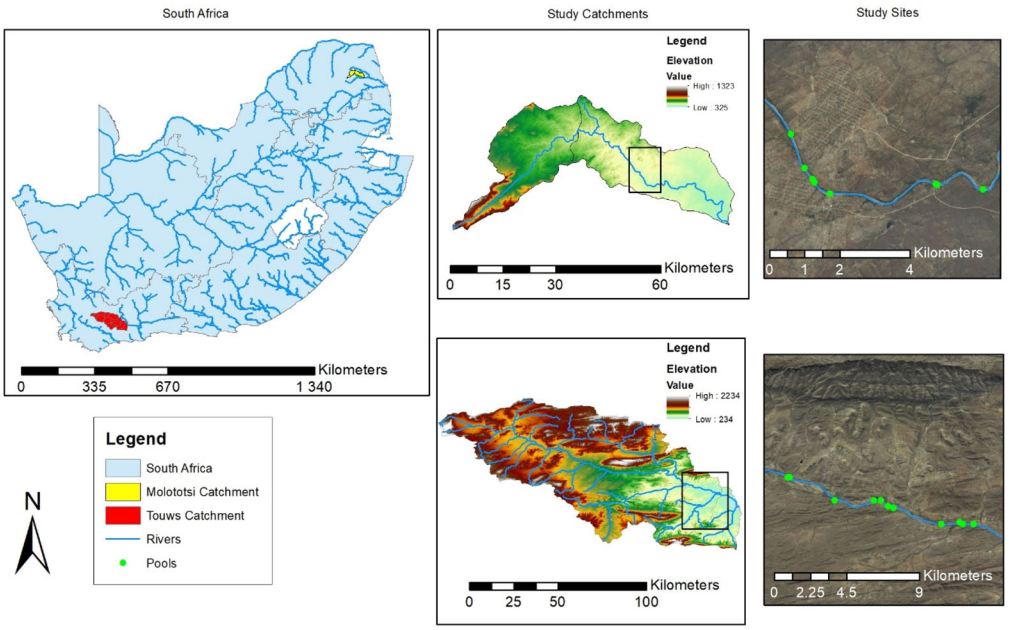

Figure 1. Location of the monitored pools along the Molototsi and Touws River catchments.

2. Study sites

The study was conducted in two NPRs found in two different catchments in South Africa. The two NPRs included the Touws and Molototsi River systems, located in the Western Cape and in the Limpopo Provinces in South Africa, respectively. The Touws river (Figure 1) is sandy-gravel above Adolpaspoot formation shale. The majority of the pools in this non-perennial river are associated with bedrock outcrop (Hattingh 2020) (Figure 2). Grenfell et al. (2021) and Hattingh (2020) provided the geomorphological account of how the pools form. The catchment is mainly covered with natural vegetation, predominantly shrubland and fynbos, with some parts of the riparian zone used for agriculture purposes. The catchment has a mean annual rainfall of 244 mm/year (Grenfell et al. 2021). The catchment received 112, 91 and 182 mm/year in 2018, 2019 and 2020 respectively, without a seasonal pattern (Figure 3). Most rainy days received less than 5 mm/d of rainfall. There were only two events that exceeded 30 mm/d. These major rainfall events produced localised flows, with some of the flows not reaching the flow station at the catchment outlet (Department of Water and Sanitation Station J1H018). According to Petersen et al. (2017), the catchment has a mean annual runoff (MAR) of 16.32 Mm^3.

The geology of the Molototsi study site (Figure 1) is predominantly characterized by the Letaba Gneiss lithostratigraphic unit, although the upper part of the catchment includes Duiwelskloof Leucogranite. The substrate of the river is sandy (Figure 2). The river is surrounded by communities (human settlements), with agriculture taking place in the riparian zone along the river. The upper catchment has a mean annual rainfall of 1219 mm/year (1998–2017) measured close to the Modjadji dam (Walker et al. 2018). However, the flood plain receives around 305 mm/yr. The catchment receives rainfall mainly during the southern hemisphere summer season between December and March (Figure 2). The upper quaternary catchment (B81G) and lower quaternary catchment (B81H) have a mean annual runoff of 16.72 and 25.84 Mm^3, respectively. Molototsi falls

Figure 2. Field photographs showing typical pools along the Molototsi (top) and Touws River (bottom).

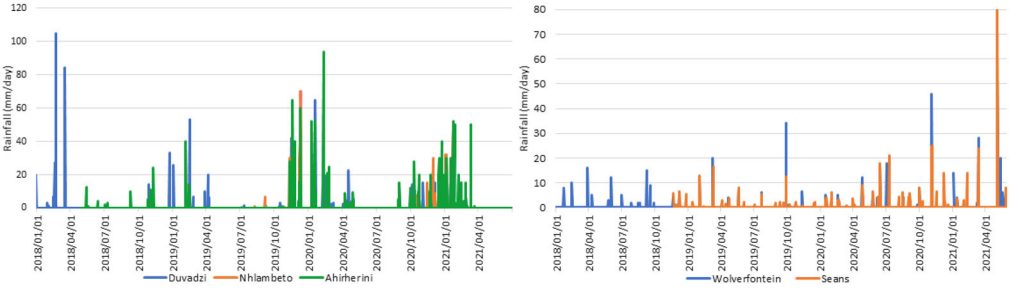

Figure 3. Rainfall data collected for Molototsi (left) and Touws River (right) catchments.

within the 2000–2500 mm/year evaporation zone (Water Research Commission (WRC) 2012) .

3. Material and methods

3.1. Remote sensing data description and collection

This study made use of open and freely available remote sensing data. The choice and selection of these data were informed by lack of high-resolution spatial data in many developing countries that cannot afford commercial satellite data sets. Sentinel-2 images

Table 1. Field visits and image acquisition dates.

Site	Field visit	Sentinel-1 image	Sentinel-2 image
Touws River	2019/07/31	2019/07/27	2019/08/01
	2020/12/14	2020/12/16	2020/12/12
	2021/03/30	2021/03/30	2021/03/28
Molototsi River	2020/01/08	[a]	[a]
	2021/06/30	2021/06/28	2021/06/30

[a]Not used because of clouds on Sentinel-2.

were therefore used. Sentinel-2 comprises twin polar-orbiting satellites in the same orbit, phased at 180° to each other. The combination of these satellites reduces the revisit time from 10 days of each satellite to 5 days at the equator and 2–3 days at mid-latitudes. Sentinel-2 has 13 spectral bands in total, four bands at 10, six at 20 m and three at 60 m spatial resolution. Sentinel-2 data are provided at different pre-processed level (1B, 1 C and 2 A) products for users. The data were acquired from USGS earth explorer (http://earthexplorer.usgs.gov/ accessed on 8 August 2020) and the Copernicus (https://scihub.copernicus.eu/ accessed on 8 August 2020) website. The level 1 C data were downloaded from the USGS website throughout the study duration.

Further, this study included SAR data obtained by Sentinel-1 to overcome the cloud-induced challenges of optical remote sensing. Sentinel-1 has C-band imaging operating in 4 modes (strip map, interferometric-wide swath, extra-wide swath and wave modes). This band can reach down to 5 m and coverage swath up to 400 km. Each satellite has a 12-day revisit time at the equator, the revisit time is bettered by the two satellites (Sentinel-1A and Sentinel-1B) orbiting in the same plane (~700 km above the earth), resulting in a revisit time of 6 days. For the Sentinel-1, SAR data under interferometric wide-swath (IW) mode were downloaded from the National Aeronautics and Space Administration Alaska Satellite Facility (NASA/ASF) (https://search.asf.alaska.edu/#/). In total, eight images with dates closest to the field surveys were used for accuracy assessment (Table 1). The use of Sentinel was informed by its performance in water resources and other related environmental applications (Kwang et al. 2017; Seaton et al. 2020). Literature has shown that Sentinel-2 performs better than Landsat 8 and has a better spatial and temporal resolution. For example, Seaton et al. (2020) highlighted that clouds are problematic for extraction of water areas using Sentinel-2 (optical remote sensing), as they reduce the number of observations, hence the need to use Sentinel-1 data (Seaton and Dube 2021).

3.2. Field data collection

During field visits, global positioning system (GPS) measurements were collected along the edges of the pools (boundary of water and non-water) in the study areas using a hand-held GPS. The accuracy level was within five metres for all collected points and approximately three metres apart (Figure 4). To assess the factors that control the changes in pool sizes, additional hydrometeorological data were needed. A few datasets including rainfall and flow occurrence obtained from the local community were used. Weather station data were obtained from the Agricultural Research Council. Landcover data were obtained from the National Geographic Institute (NGI) of South Africa. Groundwater levels were continuously measured using dataloggers in the vicinity of the pools and river.

Figure 4. Example of the field-collected points using a GPS in the Touws River on a Google Earth map.

3.3. Pool extraction from satellite data

Two methods were used to derive the spatial distribution of pools along NPRs. Field surveys and satellite images were used to identify and determine the locations of pools and pool sizes. Various remote sensing derivates were tested; these included the MNDWI, NDWI, NDVI and random forest classification derived from Sentinel-2 images and Sentinel-1 SAR data. To understand pools and pool dynamics, rainfall, flow occurrence, groundwater levels and evaporation rates were integrated. A detailed summary of the methods is summarised in Figure 5.

3.3.1. Sentinel-2 pre-processing and analyses

Pre-processing and analysis of satellite images were conducted to detect water bodies/features. Seaton et al. (2020) compared atmospheric correction methods (Sen2Cor, DOS1, TOA), and concluded that the Top of the Atmosphere (TOA) reflectance images are the most suitable methods for Sentinel-2. Similar conclusion was made by Rumora et al. (2019). Seaton et al. (2020) further indicated that the incorporation of atmospheric correction can eliminate some of the significant water surface areas. Therefore, the TOA images were used for this study. The downloaded Sentinel-2 images were first resampled to 10 m using Sentinel Application Platform (SNAP) with Band 3 as the reference band. Water indices were used to extract water areas from the images because the method is reliable, user-friendly, efficient, and with low computation cost (Du et al. 2016). The processing was done using SNAP and ESRI ArcGIS 10.3 software.

Water indices are used to distinguish between water and non-water features. This study used the most commonly used water indices, including Normalized Difference Water Index (NDWI) (McFeeters 1996) (Eq. (1)), Modified Normalized Difference Water Index (MNDWI) by Xu (2006) (Eq. (2)), and the Normalised Differential Vegetation Index (NDVI) by Trucker (1979) (Eq. (3)).

$$NDWI = (Green - NIR)/(Green + NIR) \quad (1)$$

where Green is the green band and NIR is the near infra-red band. Pixels of water have positive values.

$$MNDWI = (Green - SWIR2)/(Green - SWIR2) \quad (2)$$

where Green is the green band and SWIR is short wave infra-red band. Pixels of water have positive values.

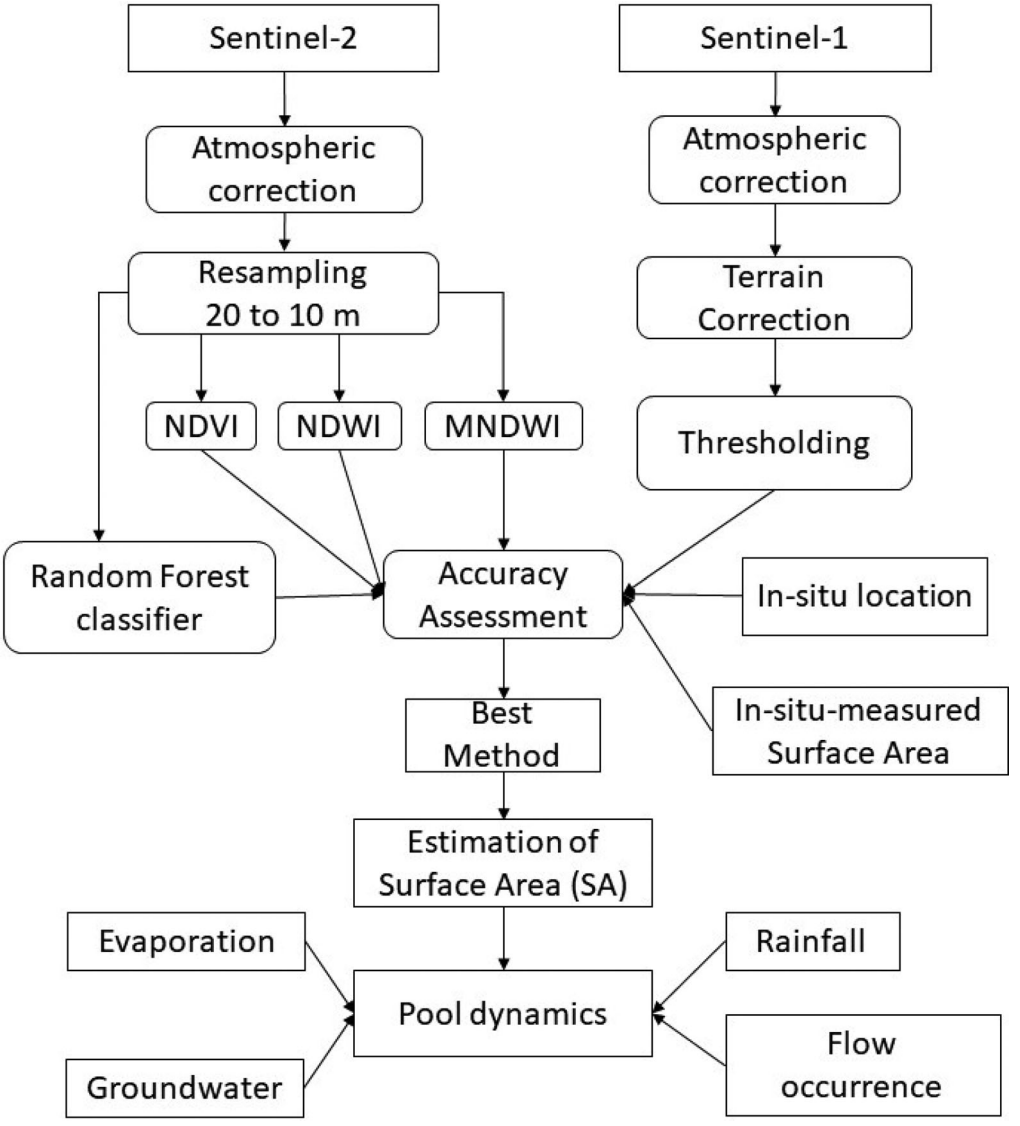

Figure 5. A flow diagram illustrating the methodological procedure used in this study.

$$NDVI = \ (NIR - Red)/(NIR - Red) \tag{3}$$

where NIR is the Near-infrared band, Red is the red band. Pixels of the water body have negative values.

The random forest classification as proposed by Breiman (2001), was also used as it is one of the commonly used methods and has been proven to produce higher accuracy in the extraction of water areas than other supervised classifiers (Ko et al. 2015; Acharya et al. 2018; Kalaivani et al. 2019). Random forest classification is an ensemble classification that produces multiple decision trees using a randomly selected subset of training images. In this case, the pools that were assessed were excluded from the training set.

Table 2. Confusion matrix used for accuracy assessment.

		Reference data	
		Water	Non-water
Classified data	Water	True positive	False positive
	Non-water	False negative	True negative

3.3.2. Shadow removal

Mountain shadows can be easily confused with water areas as they have similar spectral signatures as noted by Xu (2006). The random forest was also used to classify the areas of shadows, and an outcome raster was used to clip out areas that the indices might have confused to improve the classification accuracies.

3.3.3. Sentinel-1 pre-processing and analyses

Sentinel Application Platform (SNAP) was used for pre-processing the Sentinel-1 images. Firstly, the images were calibrated to convert raw digital numbers to the RADAR backscatter coefficient. To reduce speckle noise, the lee filter was used with a 3×3 kernel width and height. The images were aligned and corrected for elevation interference using the STRM 3 sec DEM which is auto-downloaded by the SNAP tool. Water surfaces act as mirrors and reflect almost all incoming radiation; they cause very low backscatter. Therefore, surface water detection using SAR data is often based on applying a threshold of the SAR backscatter coefficient, with low backscatter values attributed to surface water (Pham-Duc et al. 2017; Seaton and Dube 2021). Therefore, a thresholding method was used to separate water and non-water features from Sentinel-1 data. A threshold was determined for each scene, as the accuracy of Sentinel-1 in distinguishing water from other features is affected by wind-induced roughness effects, poor image quality (speckle noise) and incidence angle variance (Bioresita et al. 2018). However, based on multiple trails, the threshold used for this study was ~ -22 dB on the VH polarisation.

3.4. Accuracy assessments

3.4.1. General classification accuracy at catchment scale

Accuracy assessment was done in two folds, the one to focus on the location of the pools along the rivers and the other focused on the pool size. Random points were created and labelled based on expert knowledge of the area and high-resolution images from Google Earth Pro to obtain reference points for accuracy assessment at the catchment level. The location of the field-observed pools were also added to the random points; this was done to avoid having the random points exclusively in one class (non-water), as water bodies cover a small portion of the catchment. Pixel values were then extracted for the created points. The extracted values were then compared to the field observations. User's accuracy, producer's accuracy and overall accuracy were computed, derived from Table 2. True Positive is the number of correctly extracted water pixels, False Negative is the number of undetected water pixels, False Positive is the number of incorrectly extracted water pixels, and True Negative is the number of correctly rejected non-water pixels derived.

3.4.2. Accuracy assessment of remotely-sensed pool's surface area

The accuracy of the detection of pools was examined to determine the method to be used for pool dynamics (time series). Two representative pools were selected at each of the study catchments. The pools were selected based on the feasibility to monitor using satellite images, determined by pre-inspection. The variation in the riverbed material (bedrock,

Table 3. Detection of pools along the Touws (A) and Molototsi River (B).

Touws River (A)							
Pool name	Surface Area	Depth	MNDWI	NDWI	NDVI	RF	S1
Touwsberg Farm 1	237.8	0.41	UD	UD	UD	UD	UD
Touwsberg Farm 2	9694.5	0.94	Detected	Detected	Detected	Detected	Detected
Sean	697.2	0.3	Detected	Detected	UD	UD	UD
Wolverfontein 1 (WW1)	4403.5	0.76	Detected	Detected	Detected	Detected	Detected
Wolverfontein 2 (WW2)	7198	1.3	Detected	Detected as one	Detected	Detected	Detected
Touwsberg Office 1	158.4	0.4	UD		UD	UD	UD
Touwsberg Office 2	27,500	0.9	Detected		Detected	Detected	Detected
R62Bridge	413	0.46	UD	Detected	Detected	UD	UD
JJ1	680	1.4	Detected	Detected	UD	UD	UD
JJ2	1640	0.75	Detected	Detected	UD	UD	UD
Die sand	166.4	0.17	UD	Detected	UD	UD	UD
Molototsi River (B)							
Pool name	Surface Area	Depth	MNDWI	NDWI	NDVI	RF	S1
Mol_pool 1	127	0.28	UD	UD	UD	UD	UD
Mol_pool 2	578	0.3	UD	UD	UD	UD	UD
Mol_pool 3	3448	0.46	Detected	Detected	Detected	Detected	UD
Mol_pool 4	2880	0.43	Detected	Detected	Detected	Detected	UD
Mol_pool 5	337	0.35	UD	UD	UD	UD	UD
Mol_pool 6	590	0.52	UD	Detected	UD	UD	UD
Mol_pool 7	111	0.29	UD	UD	UD	UD	UD
Mol_pool 8	190	0.28	UD	UD	UD	UD	UD

*UD = undetected.

sand, gravel) was taken into account in order to determine how the underlying material affects the pool's storage. Proximity to hydrometeorological monitoring stations was also considered in the selection of pools. Accessibility, in terms of roads and permission, was considered. The digitised field boundary of the pools was used as reference data. The buffer technique proposed by Brovelli et al. (2015) was applied to develop a confusion matrix (Table 2) for the accuracy assessments. All pixels within the boundaries of the surface water bodies digitised were known to be water pixels. All pixels within the area of the buffer were known to be non-water pixels.

3.4.3. Assessing the difference between the observed and remotely-sensed surface area of pools

The surface water areas of the selected pools were measured during the field visits. These were then compared to the sizes obtained from the remote sensing using the Differential Area Index (DAI) also referred to as the deviation. DAI is a dimensionless index used to compare true area and estimates (Sawunyama et al. 2006; Acharya et al. 2018). In this study, DAI was used to get standardised differences between the observed area and the estimated area of pools by remote sensing approaches (Eq. (4)). The DAI values range from −1 to 1, with 0 being the perfect score indicating total agreement and −1 and 1 being the worst scores, negative indicates underestimation and positive indicates overestimation (Acharya et al. 2018). In this study, we multiplied the DAI by 100 to obtain Percentage DAI, which allows for a standardised comparison.

$$\mathrm{DAI} = (\mathrm{Ao} - \mathrm{Ae})/\mathrm{Ao} \times 100 \tag{4}$$

where Ao is the observed area and Ae is the estimated area.

3.4.4. Changes in the sizes of the selected pools

Based on the performance of the methods, the most suitable methods were used to estimate the changes in surface area of the pools from 2019 to 2021. A total of 27 images

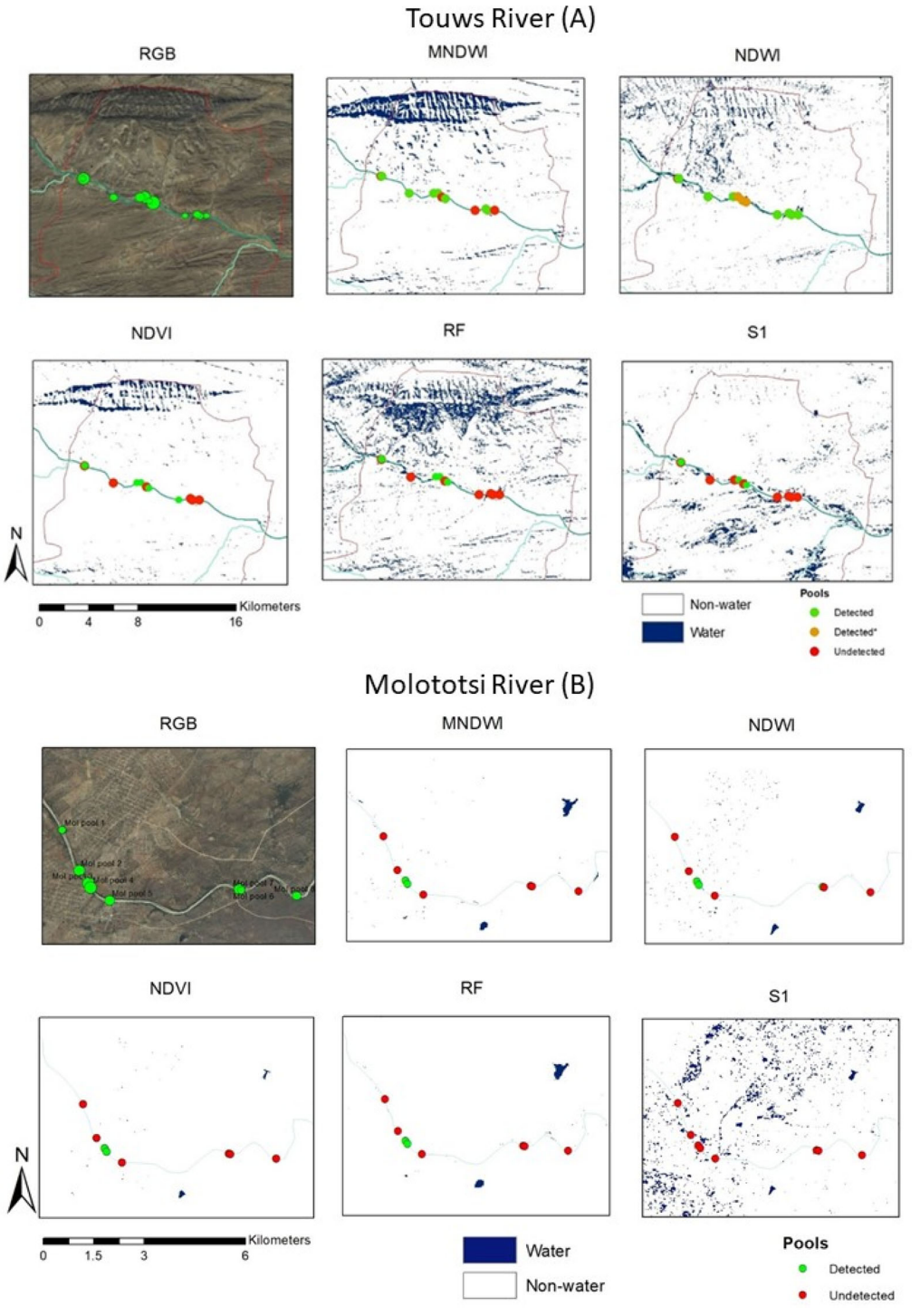

Figure 6. Performance of the methods in detection water surfaces along the Touws (A) and Molototsi River (B). Green dots indicate detected pools, red dots show undetected pools, and orange dots show two or more pools that were detected as one.

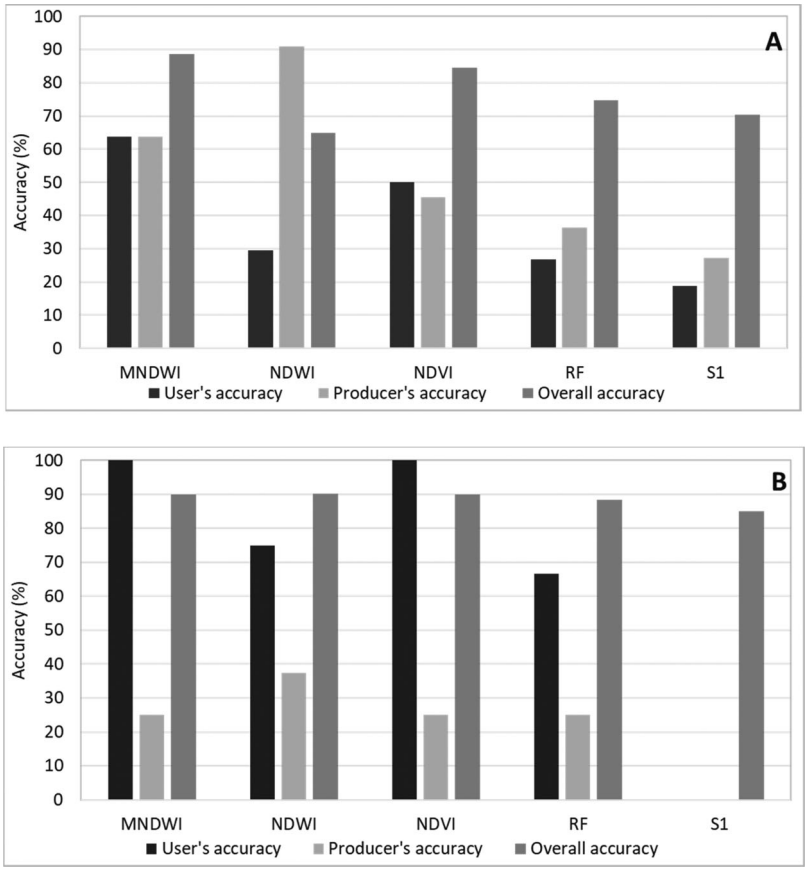

Figure 7. Accuracy of the methods in distinguishing water and non-water features at catchment scale in the Touws (A) and Molototsi River (B).

were used, these were selected to represent different phases, from when the pool is full to its driest state. Rainfall, flows occurrence, evaporation rates and groundwater levels were used to explain the factors that affected the changes in pools sizes.

4. Results

4.1. Detection of pools along Touws and Molototsi Rivers at catchment scale

Remote sensing methods were able to detect the pools along NPRs, although the accuracy of the results varied with methods and site. In the Touws River, when the MNDWI was applied on the Sentinel-2 image, 7 out of 11 pools were detected (Table 3). All pools that were not detected were relatively small (>400 m^2) in size. The NDWI detected 10 of the 11 pools, however, it detected most parts of the river as water (Figure 6).This is evident from the high producer's accuracy and the poor user's accuracy (Figure 6). NDVI was able to detect the five largest pools. Random forest classification and the Sentinel-1(S1) thresholding correctly detected four of largest pools. Along the Molototsi River, the eight surveyed pools had an average size of 1033 m^2 and an average depth of 0.3 m. NDWI detected 3 out of 8 pools. MNDWI, NDVI and supervised classification (RF) detected 2 of the 8 pools, whereas the thresholded-Sentinel-1 did not detect any of the pools. The

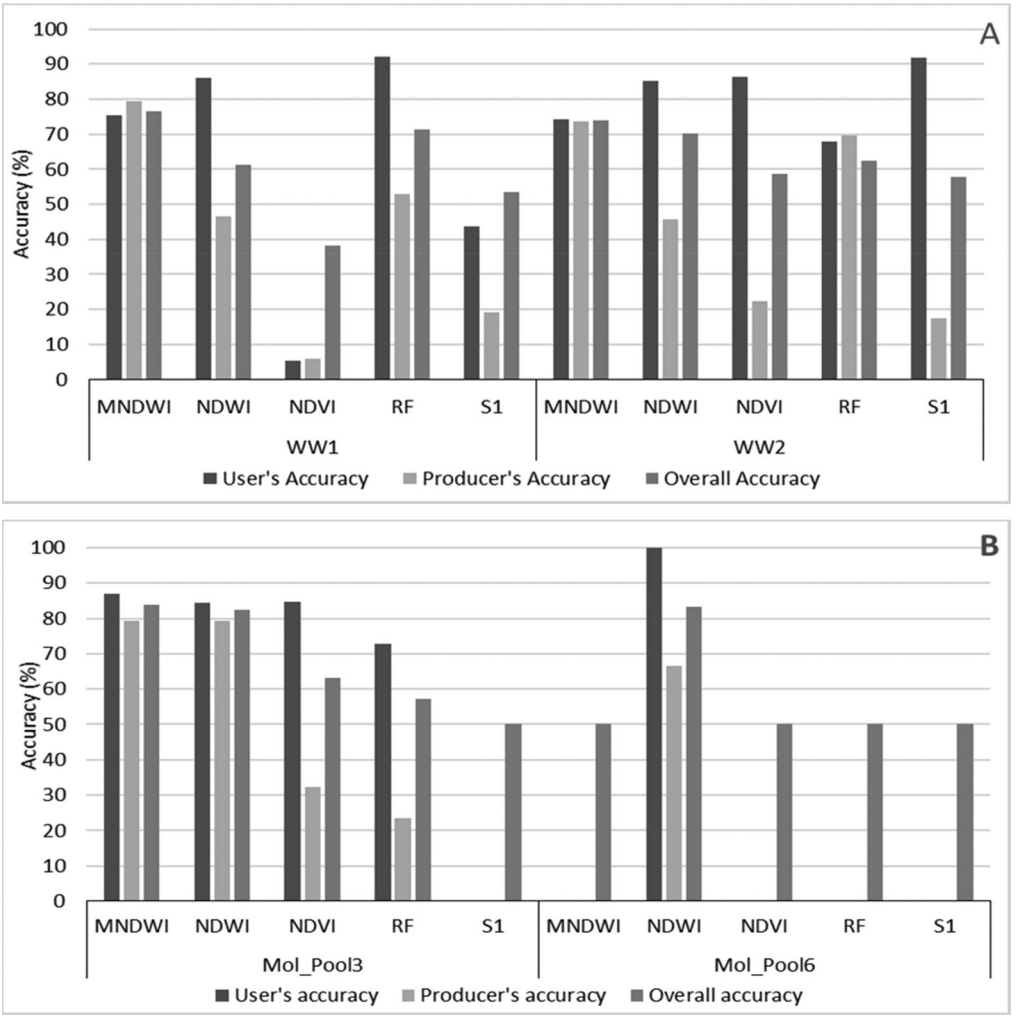

Figure 8. Performance by MNDWI, NDWI, NDVI, RF and S1 in the classification of pools in Touws (A, WW1 and WW2-Wolverfontein 1 and 2 pool) and Molototsi River (B, Pool 3 and 6).

poor detection of pools in this study site can be attributed to the size of pools, the majority of which were fairly small. The methods failed to detect the smaller pools as it was the case for the Touws River. The estimates in the Molototsi study area did not show an overestimation (noise) of water surface areas (Figure 5).

Overall, the adopted remotely-sensed methods were able to distinguish between water (pools) and non-water pixels (roads, buildings, mountainous shadows, vegetation, bare land) for the two study sites. MNDWI outperformed other methods (Overall Accuracy = 89%), whereas NDWI had high score for user's accuracy (Figure 6). The NDVI had the ability to distinguish between water and non-water pixels. The thresholded Sentinel-1 (S1) data had the worst performance with user's and producer's accuracy of less than 30%. For pools in the Molototsi area, high user's and overall accuracy were obtained; this shows that water and non-water pixels could be mapped with high accuracy (Figure 7). However, the low producer's accuracy scores were recorded for all methods due to failure

Table 4. Percent Differential Area Index for three surveys in Touws (A, pool WW1 and WW2) and one survey Molototsi (B, pool 3 and 6).

Touws River (A)				
WW1 pool				
MNDWI	**NDWI**	**NDVI**	**RF**	**S1**
−25.7	−71.4	−8.6	−31.4	85.7
6.1	78.8	100.0	53.0	43.4
1.5	81.8	100.0	87.9	77.5
WW2 pool				
MNDWI	**NDWI**	**NDVI**	**RF**	**S1**
−28.9	58.5	65.5	−31.7	96.2
26.2	74.6	93.1	50.0	71.0
−11.3	27.4	68.9	22.6	70.2
Molototsi River (B)				
Mol_Pool 3				
MNDWI	**NDWI**	**NDVI**	**RF**	**S1**
8.8	5.9	61.8	67.6	100.0
Mol_Pool 6				
MNDWI	**NDWI**	**NDVI**	**RF**	**S1**
100.0	−33.3	100.0	100.0	100.0

to detect the smaller pools, as these were predominant in this study area. The MNDWI and NDVI performed better than the other methods, and Sentinel-1 was the worst.

4.2. Accuracy assessment of remotely sensed pools' surface areas in the Touws and Molototsi River

The surface areas obtained with MNDWI, NDWI, NDVI and RF applied to Sentinel-2 image and Sentinel-1 threshold (S1) were compared to the field obtained surface areas. Random forest classification and thresholding of Sentinel-1 had the highest user's accuracy (92%) for the WW1 and WW2 pool (described in Table 3), respectively. Overall, MNDWI outperformed the other methods as it had acceptable accuracies for all three accuracy measures for both pools, ranging from 74% to 80% (Figure 8). When comparing the scores from the two pools, the WW1 pool size was better estimated. Field survey was done from 30 June to 1 July 2021 along the Molototsi River. The MNDWI slightly outperformed the other methods for Pool 3 (Figure 8), whereas NDWI was the only method that detected Pool 6. S1 had the worst performance as it did not detect both pools. Comparing the extraction of the two pools, Pool 3 was better extracted when all methods are considered.

4.2.1. The difference in observed and estimated surface areas of pools

The pool areas estimated with remote sensing tended to be overestimated for both pools (Table 4). Further, the MNDWI showed lower errors when estimating the surface water area of pools, as it outperformed all other methods, in one instance the difference was 1.5%. The thresholded Sentinel-1 data and NDVI showed high differences/errors ranging from 43% to 100%, although NDVI had the best estimate for the WW1 pool on one occasion (PDAI = −8.6%). When comparing the estimates for the two Touws pools, the WW1 pool was better estimated. For the Molototsi pools, NDWI showed lower errors when estimating the surface water area of pools, as it outperformed all other methods, with PDAI of 5.9% and 33.3% for Pool 3 and Pool 6, respectively. The thresholded Sentinel-1 data had the highest errors of 100% for both pools, indicating that pools were not detected. When comparing the estimates for the two Molototsi pools, Pool 3 was better estimated.

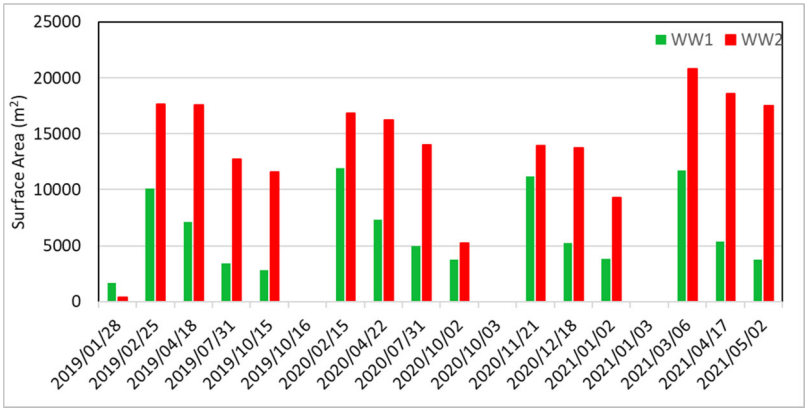

Figure 9. Changes of the surface water area of WW1 (green bars) and WW2 (red bars) in the Touws River when full, at intermediate and dry stage.

4.3. Changes in pool sizes and factors that control the changes in Touws and Molototsi Rivers

There were four major flow events in Touws river from 2019 to May 2021. The maximum surface water area estimated was 12,000 m^2 and 20,800 m^2 for WW1 and WW2 pools, respectively (Figure 9). The maximum surface area was stable for WW1 but fluctuated for the WW2 pool, possibly due to errors of WW2 detection. During the study period (2019–2021), the pools were at the driest level in January 2019 with surface areas of 1600 and 400 m^2 for WW1 and WW2, respectively. This was after 2 years of no river flows. This was followed by October 2020 when the pools had surface water areas of 3700 and 5200 m^2 for WW1 and WW2, respectively. This was after six months without significant inflows. Compared to Touws, Molototsi had two major flow events during the summer season of each year. The pools were present at the end of flow events in February/March and dried out in June/July of each year (Figure 10). The maximum surface water area was estimated to be 2900 m^2 and 1300 m^2 in Pools 3 and 6, respectively. Pool 3 was completely dry in 2020 and did not exist in 2019. Pool 6 dried up in June 2020, and it was almost completely dry in June 2021 with a surface water area of 100 m^2.

The remotely sensed estimates of surface water area correlate well with rainfall and flow occurrence for the Touws River (Figure 11). After flow events, the surface area of the pools increased to maximum size. The flow event marked with red occurred downstream of the WW1 pool, therefore it did not affect the size of the WW1 pool. Rainfall adds water that maintains the pools, delaying the drying up of pools. The surface area of pools decreased after the major inflow; this means some losses occurred. Both shallow and deep groundwater levels did not show any notable changes in relation to the surface area of the pools, rainfall and the occurrence of flow. This suggests that there might be no vertical interaction between the pools and the groundwater system. This indicates that water is lost to the atmosphere through evaporation and to the unsaturated zone. Potential evaporation at the site was 94 and 82% higher than rainfall in 2019 and 2020, respectively. Evaporation, therefore, plays a significant role in water losses. These patterns were observed for the two pools, although the maximum size of the WW2 pool fluctuated and should have been affected by the event that occurred in October 2019, however, there was no increase in the size of the pool (Figure 10).

In the Molototsi site, remotely sensed estimates of the surface water area correlated well with rainfall and the occurrence of flow for Pool 6 (Figure 12). Rainfall added water

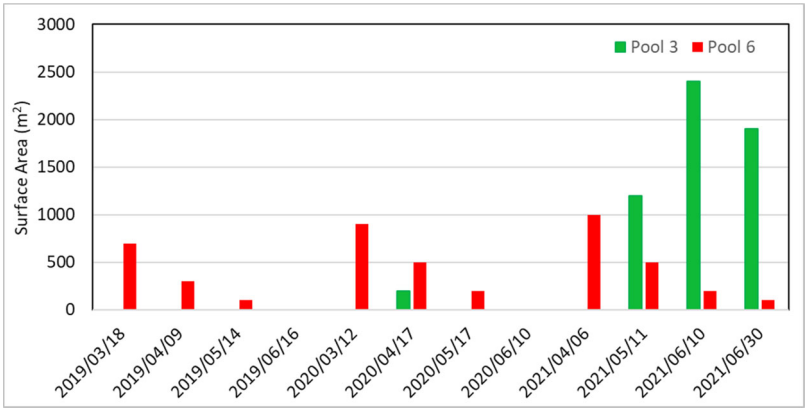

Figure 10. Changes of the surface water area of Pool 3 (green bars) and Pool 6 (red bars) in the Molototsi River when full, at intermediate and dry stage.

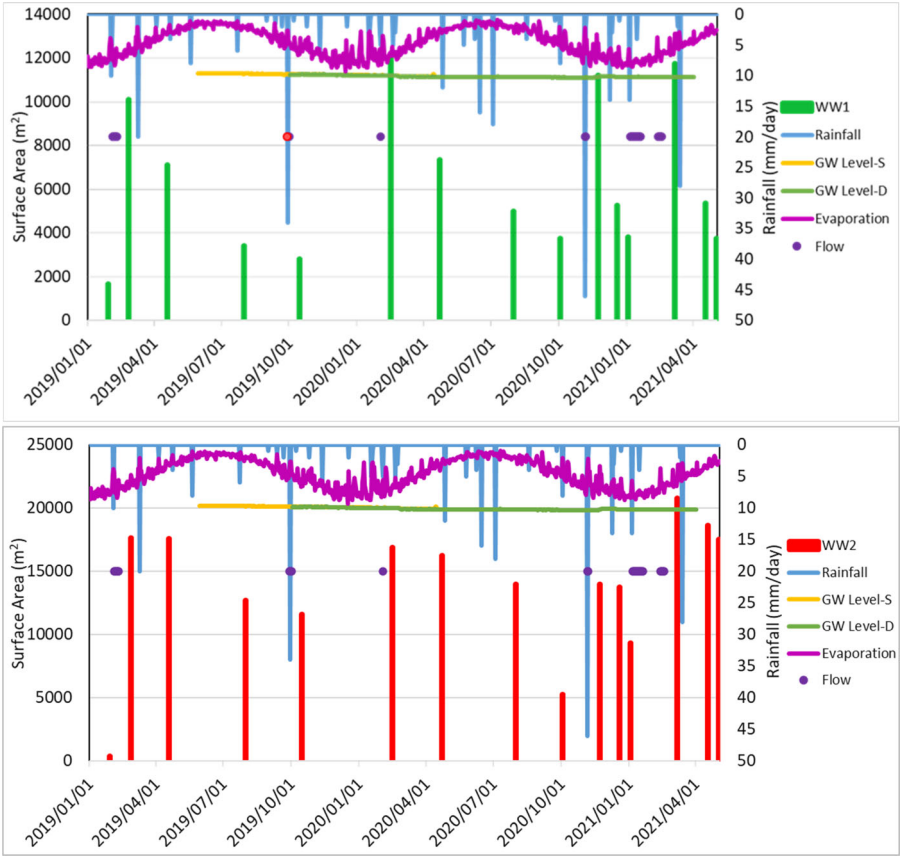

Figure 11. Changes of the surface water area of WW1 (green bars), WW2 pool (red bars), with daily rainfall (blue line), the occurrence of flow (purple dot), shallow (orange line) and deep (green line) groundwater levels, evaporation (purple line).

that maintained the pool, delaying the drying up of the pool. The surface area of pools decreased after the major inflow; this means some losses occurred. Groundwater levels did not show any notable changes in relation to the surface area of the pools, rainfall and

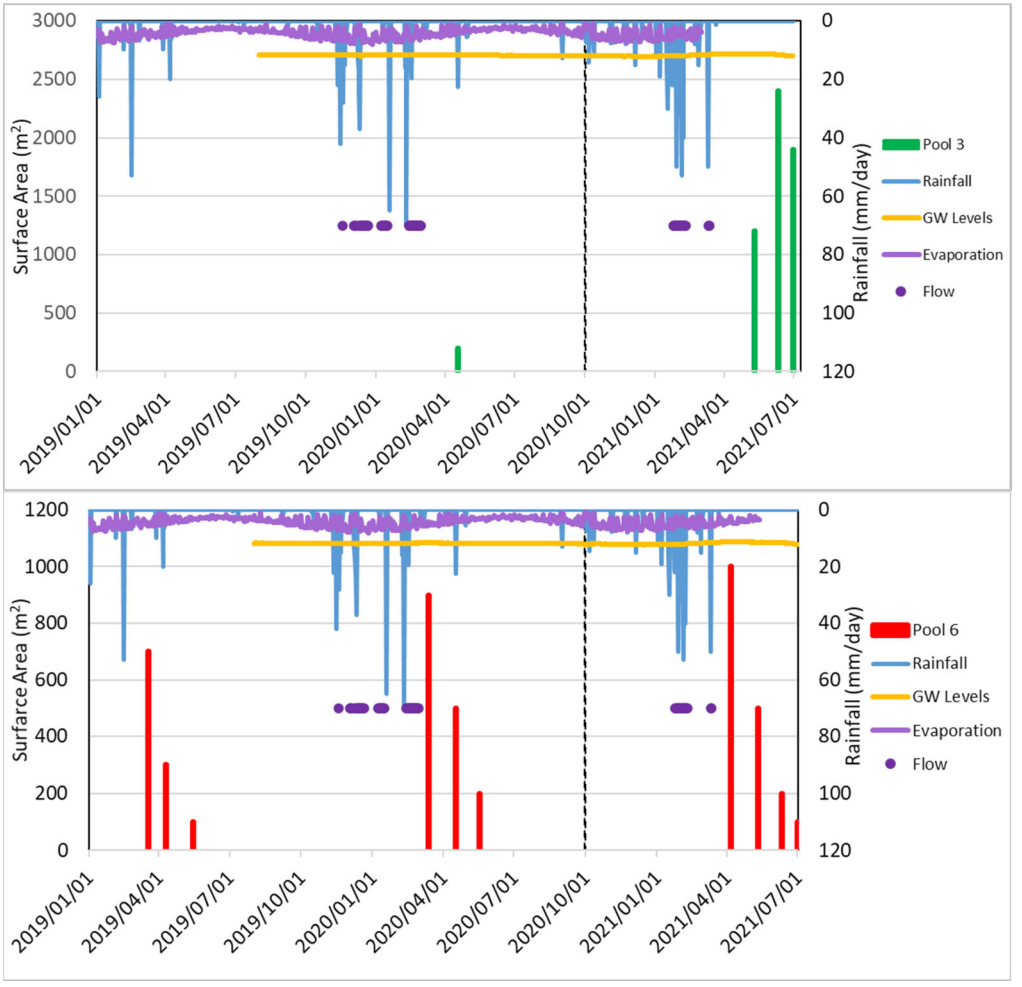

Figure 12. Changes of the surface water area of Pool 3 (green bars) and Pool 6 (red bars), with daily rainfall (blue line), the occurrence of flow (purple dot) and groundwater levels (orange line). The black dashed line indicates the start of groundwater pumping on the site.

flow occurrence, suggesting that there might not be vertical interaction between the pools and groundwater system. This suggests that water is lost to the atmosphere through evaporation and to the unsaturated zone. In this area, potential evaporation was 77 and 75% more than rainfall received in 2019 and 2020, respectively. There was no evident relation between rainfall and Pool 3. Other factors such as river sand mining and water withdrawals from the river might have influenced its sizes.

5. Discussion

This study explored the use of remote sensing in monitoring the spatial distribution of pools and pool dynamics along non-perennial rivers in two distinct areas. The results showed that the pools in Touws River were bigger than pools in the Molototsi River. This might be due to the Molototsi River having sandy bed material with high hydraulic conductivity draining water after flash floods (Walker et al. 2018). In contrast, the Touws

River has bedrock that is not far from the river bed, hence it is classified as a mixed alluvial and bedrock river (Grenfell et al. 2021). Furthermore, Molototsi has a clear dry and wet season, whereas the Touws River receives rainfall and flows at any time of year. However, the use of remotely sensed data demonstrated the capability to detect pools at both river and pool scale.

In both rivers, pools with shallow water (depth of approx. 0.3 m) were detected, but those that were small in surface area were not detected. The failure to detect pools with small surface areas may be due to the satellite image resolution, where pixels including small pools are detected as non-water. The MNDWI and NDWI detected pools better than other methods in both Touws and Molototsi Rivers, respectively. However, the MNDWI did not detect pools that were smaller than 400 m^2. This is due to the short wave infrared band of Sentinel-2 having a slightly coarser spatial resolution (20 m). Resampling it to 10 m did not make a difference, whereas the NDWI uses bands that have a 10 m spatial resolution and it was able to detect some pools that are less than 400 m^2. Li et al. (2021) made the same observation when mapping a small river. The NDWI is known to have challenges in separating shallows and built-up areas (Bangira et al. 2019). This might explain why the index did not outperform MNDWI on the mountainous Touws River site as compared to the relatively flat Molototsi site. All this also suggests that the small pools require better resolution imagery in order to be detected.

The random forest classification detected the pools with acceptable accuracy; however it did not meet expectations at both catchment and pool scale. This might be because pools tend to have different characteristics that affect the training of the classifier, such as the presence of algae, vegetation, sediments in the pools, and the size and shape of the pool. Even parts of pools can have different spectral signatures. All these might have limited the detection of pools by the random forest classifier as there are usually few water bodies that can be used to train the classifier in these dry areas. As a result, the training might not be diverse enough to capture the differences found in pools. Bangira et al. (2019) state that this is the disadvantage of machine learning classifiers. Sentinel-1did not perform well compared to results obtained from Sentinel-2. This is similar to results obtained by Bangira et al. (2019). Although Sentinel-1 had been applied to mapping floods over large areas, it was not suitable for detecting pools at both study sites. For an index that was produced to detect vegetation, NDVI performed well in both catchments.

When comparing the accuracy at the pool's size scale in Touws River, the WW1 pool was estimated better than the WW2 pool. All methods had difficulty in classifying the pixels around the WW2 pool due to the shadow in the morning, the time of day when Sentinel-2 captures images. To reduce this misclassification, the random forest classifier was trained for the hill shadows, thereafter, some misclassified pixels were removed. Pool 3, which was the largest pool in the Molototsi River, was also detected better than Pool 6. However, only the NDWI was able to detect Pool 6.

In both catchments, the surface area of the pools generally correlated well with the occurrence of flows and rainfall with the exception of one flow event that did not match the change in surface area of the WW2 pool. The results showed no notable responses of groundwater levels to surface water area of the pools, nor to rainfall and river flows. This can be attributed to the nature of the underlying geology of the study sites, shale for Touws and gneiss rock for Molototsi. This suggests that the pools are not losing water to the groundwater system. These findings differ from many studies that have indicated that groundwater sustains the pools (Bestland et al. 2017; Lamontagne et al. 2021). However, Walker et al. (2018) made the same finding in the Molototsi catchment using water levels

and geochemical analyses. Hamilton et al. (2005) reported similar findings for pools in Australia, adding that clay found at the bottom of pools can also contribute in reducing the interaction between groundwater and pools.

The results imply that altering the flow regime will significantly affect the spatial distribution of pools and pool dynamics. The pools are not only important water sources for the surrounding communities but they also provide habitat and maintain the aquatic life of the river (Bonada et al. 2020). Further, they improve food security in the surrounding communities (Sustainable Development Goal 2) as complete drying of pools may result in total loss of aquatic life, including fish (Marshall et al. 2016). The results also showed that pools at the study sites might not be sensitive to groundwater abstraction.

6. Conclusion

The study demonstrated the potential of using remote sensing methods to determine the spatial distribution and dynamics of pools in two contrasting non-perennial rivers, the one characterized by sandy-gravel bed with pools associated with bedrock outcrops (Touws River) and the other exhibiting a sandy alluvium with pools migrating following flow events (Molototsi River). Remotely-sensed methods detected pools with acceptable accuracy in both rivers, except for small pools ($<400\,m^2$). Overall, MNDWI performed better than other methods in the mountainous Touws River, whereas NDWI performed better in the relatively flat Molototsi flood plain. The pools in the Touws River showed a perennial pattern, whereas pools in the Molototsi River showed ephemeral behaviour persisting only for a few months after flows. Rainfall and flow occurrences are key in controlling temporal changes in pools sizes, and there was no evidence of interaction between pools and groundwater in both rivers. Water balance analysis, however, may be able to clarify, to a greater extent, how these fluxes are responsible for the changes over time in pools.

Remote sensing proved be a useful approach to record water occurrence and availability in poorly monitored non-perennial rivers. It is suggested that this approach could be used to fill ground monitoring gaps in non-perennial rivers and it could be incorporated in national hydrological monitoring networks. Water available in non-perennial river pools can be considered an important water resource in semi-arid environments. If properly managed, this additional water resource could serve to provide water for livestock and domestic purposes in rural communities. It also provides ecohydrological services such as flood attenuation and storage of floodwaters, as well as habitats, feeding and spawning ground for various aquatics species, thereby indirectly supporting the tourism sector and livelihoods.

Acknowledgements

We would like to appreciate the Water Research Commission of South Africa for funding this project (K5/2936) and the University of the Western Cape for providing us with the opportunity to do this work.

ORCID

T. Dube http://orcid.org/0000-0003-3456-8991

Data availability statement

The data that support the findings of this study are available on request from the corresponding author. The data are not publicly available due to restrictions by a third party.

Disclosure statement

No potential conflict of interest was reported by the authors.

References

Acharya TD, Subedi A, Lee DH. 2018. Evaluation of water indices for surface water extraction in a landsat 8 scene of Nepal. Sensors (Switzerland). 18(8):2580.

Bangira T, Alfieri SM, Menenti M, van Niekerk A. 2019. Comparing thresholding with machine learning classifiers for mapping complex water. Remote Sens. 11(11):1351.

Bestland E, George A, Green G, Olifent V, Mackay D, Whalen M. 2017. Groundwater dependent pools in seasonal and permanent streams in the Clare Valley of South Australia. J Hydrol Reg Stud. 9:216–235. http://doi.org/10.1016/j.ejrh.2016.12.087.

Bioresita F, Puissant A, Stumpf A, Malet JP. 2018. A method for automatic and rapid mapping of water surfaces from Sentinel-1 imagery. Remote Sens. 10(2):217.

Bonada N, Cañedo-Argüelles M, Gallart F, von Schiller D, Fortuño P, Latron J, Llorens P, Múrria C, Soria M, Vinyoles D, et al. 2020. Conservation and management of isolated pools in temporary rivers. Water (Switzerland). 12(10):1–24.

Bourke S, Shanafield M, Hedley P, Dogramaci S. 2020. A hydrological framework for persistent river pools in semi-arid environments. Hydrol Earth Syst Sci Discuss. (April):1–18.

Breiman L. 2001. Random Forests. Mach. Learn. 45(1):5–32.

Brovelli MA, Molinari ME, Hussein E, Chen J, Li R. 2015. The first comprehensive accuracy assessment of global and 30 at a national level: methodology and results. Remote Sens. 7(4):4191–4212.

Datry T, Bonada N, Boulton AJ. 2017. Intermittent Rivers and ephemeral streams: ecology and management. London: Academic Press.

Davis J, Pavlova A, Thompson R, Sunnucks P. 2013. Evolutionary refugia and ecological refuges: key concepts for conserving Australian arid zone freshwater biodiversity under climate change. Glob Chang Biol. 19(7):1970–1984. http://doi.org/10.1111/gcb.12203.

Du Y, Zhang Y, Ling F, Wang Q, Li W, Li X. 2016. Water bodies' mapping from Sentinel-2 imagery with Modified Normalized Difference Water Index at 10-m spatial resolution produced by sharpening the SWIR band. Remote Sens. 8(4):354.

Grenfell MC, Grenfell SE, Mazvimavi D. 2021. Morphodynamic modelling of dryland non-perennial riverscapes, with implications for environmental water allocation. Prog Phys Geogr. 45(5):1–32.

Groves CR, Game ET, Anderson MG, Cross M, Enquist C, Ferdaña Z, Girvetz E, Gondor A, Hall KR, Higgins J, et al. 2012. Incorporating climate change into systematic conservation planning. Biodivers Conserv. 21(7):1651–1671.

Hamilton SK, Bunn SE, Thoms MC, Marshall JC. 2005. Persistence of aquatic refugia between flow pulses in a dryland river system (Cooper Creek, Australia). Limnol Oceanogr. 50(3):743–754.

Hattingh KJ. 2020. Geomorphological controls on pool formation and pool persistence in non-perennial river [MSc Dissertation]. University of the Western Cape. August 2020.

Hughes DA. 2005. Hydrological issues associated with the determination of environmental water requirements of ephemeral rivers. River Res Appl. 21(8):899–908. http://doi.org/10.1002/rra.857.

Ilhéu M, da Silva J, Morais M, Matono P, Bernardo JM. 2020. Types of dry-season stream pools: environmental drivers and fish assemblages. Inl Waters [Internet]. 10(4):516–528.

Kalaivani K, Phamila AV, Selvaperumal SK. 2019. Random forest classifier for extracting water bodies from pansharpened image to detect surface water changes. IJEAT. 9(1):4910–4915.

Ko BC, Kim HH, Nam JY. 2015. Classification of potential water bodies using landsat 8 OLI and a combination of two boosted random forest classifiers. Sensors (Basel). 15(6):13763–13777.

Kwang C, Osei Jr EM, Amoah AS. 2017. Comparing of landsat 8 and sentinel 2A using water extraction indexes over Volta River. JGG. 10(1):1.

Lamontagne S, Kirby J, Johnston C. 2021. Groundwater–surface water connectivity in a chain-of-ponds semiarid river. Hydrol Process. 35(4):1–11.

Li J, Wang C, Xu L, Wu F, Zhang H, Zhang B. 2021. Multitemporal water extraction of dongting lake and poyang lake based on an automatic water extraction and dynamic monitoring framework. Remote Sens. 13(5):865.

Liu J, Zhang C. 2017. Identification of risks and estimation of flood storage in ponds. Math Probl Eng. 2017:1–9.

Makwinja R, Chapotera M, Likongwe P, Banda J, Chijere A. 2014. Location and roles of deep pools in Likangala river during 2012 recession period of Lake Chilwa basin. Int J Ecol. 2014:1–4.
Marshall JC, Menke N, Crook DA, Lobegeiger JS, Balcombe SR, Huey JA, Fawcett JH, Bond NR, Starkey AH, Sternberg D, et al. 2016. Go with the flow: the movement behaviour of fish from isolated waterhole refugia during connecting flow events in an intermittent dryland river. Freshw Biol. 61(8): 1242–1258.
Maswanganye SE, Dube T, Mazvimavi D, Jovanovic N. 2021. Remotely sensed applications in monitoring the spatio-temporal dynamics of pools and flows along non-perennial rivers: a review. South Afr Geogr J [Internet]. 1–19.
McFeeters SK. 1996. The use of the Normalized Difference Water Index (NDWI) in the delineation of open water features. Int J Remote Sens [Internet]. 17(7):1425–1432.
Naidoo R, Brennan A, Shapiro AC, Beytell P, Aschenborn OD, Preez P, Kilian JW, Stuart-Hill G, Taylor RD. 2020. Mapping and assessing the impact of small-scale ephemeral water sources on wildlife in an African seasonal savannah. Ecol Appl. 30(8):1–12.
Peden D, Amede T, Haileslassie A, Faki H, Mpairwe D, Breugel Pv, Herero M. 2012. Livestock and water in Nile Basin. In: Bekele S, Smakhtin V, Molden D, Peden D, editors. The Nile River Basin: water, agriculture, governance and livelihoods. London: Routledge. p. 154–185.
Petersen CR, Jovanovic NZ, Le Maitre DC, Grenfell MC. 2017. Effects of land use change on streamflow and stream water quality of a coastal catchment. Water SA. 43(1):139–152.
Pham-Duc B, Prigent C, Aires F. 2017. Surface water monitoring within cambodia and the Vietnamese Mekong Delta over a year, with Sentinel-1 SAR observations. Water (Switzerland). 9(6):366.
Rodríguez-Lozano P, Woelfle-Erskine C, Bogan MT, Carlson SM. 2020. Are non-perennial rivers considered as valuable and worthy of conservation as perennial rivers? Sustain. 12(14):5782.
Rumora L, Miler M, Medak D. 2019. Contemporary comparative assessment of atmospheric correction influence on radiometric indices between Sentinel-2A and Landsat 8 imagery. Geocarto Int. 36(1): 13–27.
Sawunyama T, Senzanje A, Mhizha A. 2006. Estimation of small reservoir storage capacities in Limpopo River Basin using geographical information systems (GIS) and remotely sensed surface areas: case of Mzingwane catchment. Phys Chem Earth. 31(15–16):935–943.
Seaton D, Dube T. 2021. A new modified spatial approach for monitoring non-perennial river water availability using remote sensing in the Tankwa Karoo, Western Cape, South Africa. Water SA. 47(3): 338–346.
Seaton D, Dube T, Mazvimavi D. 2020. Use of multi-temporal satellite data for monitoring pool surface areas occurring in non-perennial rivers in semi-arid environments of the Western Cape, South Africa. ISPRS J Photogramm Remote Sens [Internet]. 167(July):375–384.
Shanafield M, Bourke SA, Zimmer MA, Costigan KH. 2021. An overview of the hydrology of non-perennial rivers and streams. Wiley Interdiscip Rev Water. 8(2):1–25.
Sheldon F, Bunn SE, Hughes JM, Arthington AH, Balcombe SR, Fellows CS. 2010. Ecological roles and threats to aquatic refugia in arid landscapes: dryland river waterholes. Mar Freshwater Res. 61(8): 885–895.
Theodoropoulos C, Papadaki C, Vardakas L, Dimitriou E, Kalogianni E, Skoulikidis N. 2019. Conceptualization and pilot application of a model-based environmental flow assessment adapted for intermittent rivers. Aquat Sci. 81(1):1–17.
Trucker CJ. 1979. Red and photographic infrared linear combinations for monitoring vegetation. Remote Sens. Environ. 8:127.
Walker D, Jovanovic N, Bugan R, Abiye T, Du Preez D, Parkin G, Gowing J. 2018. Alluvial aquifer characterization and resource assessment of the Molototsi sand river, Limpopo, South Africa. J Hydrol Reg Stud. 19(April):177–192.
Water Research Commission (WRC). 2012. Data from: water resources of South Africa, 2012 study (WR2012) [Dataset] [accessed 2021 February 21]. https://waterresourceswr2012.co.za/.
Xu H. 2006. Modification of normalized difference water index (NDWI) to enhance open water features in remotely sensed imagery. Int J Remote Sens. 27(14):3025–3033.
Zacharias I, Zamparas M. 2010. Mediterranean temporary ponds. A disappearing ecosystem. Biodivers Conserv. 19(14):3827–3834.
Zamxaka M, Pironcheva G, Muyima NYO. 2004. Bacterial community patterns of domestic water sources in the Gogogo and Nkonkobe areas of the Eastern Cape Province, South Africa. WSA. 30(3): 341–346.